Manuscript for *Revista Mexicana de Astronomía y Astrofísica* (2009)

CONSTRAINING COSMOLOGICAL INFLATION

J. Alberto Vázquez [1], Luis, E. Padilla [2,3], Tonatiuh Matos [2,3]

Draft version: December 4, 2017

RESUMEN

El objetivo de este artículo es ofrecer una introducción cualitativa a la teoría de la inflación cosmólogica y su relación con las observaciones cosmológicas. El modelo inflacionario resuelve algunos de los problemas fundamentales que desafían al modelo estándar de la cosmología (Big Bang), por ejemplo, el problema de la Planicidad, Horizonte y la inexistencia de Monopolos, y además de resolver estos problemas, explica el origen de la estructura a gran escala del Universo, como son las galaxias. Se describen las características generales de esta solución llevada a cabo por un campo escalar. Por último, con el uso de recientes (y futuros) estudios, se presentan constricciones de los parámetros inflacionarios $(n_{\rm s}, r)$ que nos permitirán realizar la conexión entre la teoría y las observaciones cosmológicas. De ésta manera, con los últimos resultados observacionales, es posible elegir o al menos limitar el modelo inflacionario correcto, parametrizado por el potencial de campo escalar $V(\phi)$.

ABSTRACT

The aim of this paper is to provide a qualitative introduction to the inflationary theory and its relation with current cosmological observations. The inflationary model solves many of the fundamental problems which challenge the Standard Big Bang cosmology i.e. Flatness, Horizon and Monopole problem, and additionally provides an explanation for the initial conditions of the Large-Scale Structure observed in the Universe, such as galaxies. In this review we describe the general properties of this solution carry out by a single scalar field. Then with the use of current and future surveys, we show the constraints imposed on the inflationary parameters $(n_{\rm s}, r)$ which allow us to make the connection between theoretical and observational cosmology. In this way, with the latest observational results, it is possible to choose or at least to constrain the right inflationary model, parameterised by the scalar field potential $V(\phi)$.

Key Words: cosmology: cosmological parameters — cosmology: observations — cosmology: inflation

1. INTRODUCTION

The Standard Big Bang (SBB) cosmology is currently the most accepted model describing the central features of the observed Universe. This model

[1]Kavli Institute for Cosmology / Cavendish Laboratory, Cambridge, UK.

[2]Departamento de Física, Centro de Investigación y de Estudios Avanzados del IPN, México.

[3]Instituto Avanzado de Cosmología (IAC), http://www.iac.edu.mx/

has been successfully proved on cosmological levels. For instance numerical simulations of structure formation of galaxies, galaxy cluster and the abundance of primordial elements are some predictions that are in good agreement with astronomical observations (Tegmark et al. 2001; Springel et al. 2005; Kolb & Turner 1994). The SBB model also predicts the temperature fluctuations observed in the Cosmic Microwave Background radiation (CMB) with a high degree of accuracy: inhomogeneities of about one part in one hundred thousand (Komatsu et al. 2011; Planck Collaboration 2016) . These two predictions, amongst many others, are the great success of the SBB cosmology. Nevertheless, when we have a closer look at different scales, there might seem to exist certain inconsistencies or unexplained features in contrast with expected by the theory. Some of these unsatisfactory aspects led to the emergence of the inflationary model (Guth 1981; Linde 1982, 1983; Albrecht & Steinhardt 1982).

In this work, we briefly present some of the relevant shortcomings the standard cosmology is dealing with, and a short review is carried out about the scalar fields as a promising solution. Moreover, it is shown how an inflationary single-field model can be completely described by only specifying its potential form $V(\phi)$. Based on the slow-roll approximation it is found that the observational parameters, which allow us to make the connexion with experiments, are given by the amplitude of density perturbation δ_H, the scalar spectral index $n_{\rm s}$ and the tensor-to-scalar ratio r. Finally, the theoretical predictions for different scalar field potentials are shown and compared with current observational data on the phase-space parameter $n_{\rm s} - r$, thus pinning down the number of candidates and making predictions about the shape of $V(\phi)$.

2. PROBLEMS WITH THE OLD COSMOLOGICAL MODEL

Before starting with the theoretical description, let us consider some assumptions on which the SBB model is built on (Coles & Lucchin 1995):

1) The physical laws at the present time can be extrapolated further back in time and be considered as valid in the early Universe. In this context, gravity is described by the theory of General Relativity without a cosmological constant (Λ), up to the Plank era.

2) The cosmological principle holds: "There do not exist preferred places in the Universe". This is telling us that the properties of the Universe at large-scale must be the homogeneity and isotropy, both of them encoded on the Friedmann-Robertson-Walker (FRW) metric

$$ds^2 = -dt^2 + a^2(t)\left[\frac{dr^2}{1-kr^2} + r^2(d\theta^2 + sin^2\theta\, d\phi^2)\right], \tag{1}$$

where (t, r, θ, ϕ) describe the time-polar coordinates; the spatial curvature is given by the constant k and the scale-factor $a(t)$ represents the physical size of the Universe, normalize up to today.

3) The anisotropic Universe is well described by a linear expansion of the metric about the FRW background:

$$g_{\mu\nu}(\mathbf{x},t) = g^{FRW}_{\mu\nu}(\mathbf{x},t) + h_{\mu\nu}(\mathbf{x},t). \tag{2}$$

To avoid long calculations and make this article accessible to young scientists, many technical details have been omitted or simplified; we encourage the reader to check out the vast amount of literature about the inflationary theory (Liddle & Lyth 2000; Liddle 1999; Kolb & Turner 1994; Dodelson 2003; Linde 1990).

To describe the general properties of the Universe, we assume its dynamics is governed by a source treated as a perfect fluid with pressure $p(t)$ and density $\rho(t)$. Both quantities may often be related via an equation of state $p = p(\rho)$. Some of the well studied cases are

$$\begin{aligned} p &= \frac{\rho}{3} && \text{radiation,} \\ p &= 0 && \text{dust,} \\ p &= -\rho && \Lambda. \end{aligned} \tag{3}$$

The Einstein equations for these kind of constituents, neglecting the cosmological constant Λ contribution, are given by:
The **Friedmann equation**

$$H^2 \equiv \left(\frac{\dot{a}}{a}\right)^2 = \frac{8\pi}{3m_{Pl}^2}\rho - \frac{k}{a^2}, \tag{4}$$

the **acceleration equation**

$$\frac{\ddot{a}}{a} = -\frac{4\pi}{3m_{Pl}^2}(\rho + 3p), \tag{5}$$

and the energy conservation for the fluids described by the **fluid equation**

$$\dot{\rho} + 3H(\rho + p) = 0, \tag{6}$$

where overdots mean time derivative, and H defines the *Hubble parameter*. Hereafter we employ natural units $c = \hbar = 1$; the Planck mass m_{Pl} is related to the gravitational constant G through $G \equiv m_{Pl}^{-2}$.

We notice from Eqn. (4) that for a particular Hubble parameter there exists a particular density for which the universe is spatially flat ($k = 0$). This is known as the *critical density* ρ_c and is given by

$$\rho_c(t) \;=\; \frac{3m_{Pl}^2\, H^2}{8\pi}, \tag{7}$$

where ρ_c is a function of time due to the presence of H. In particular, its present value is denoted as $\rho_{c,0} = 1.87840(9)\, h^2 \times 10^{-26}$ kg m^{-3}, or in terms

of more convenient units taking into account large scales in the Universe, $\rho_{c,0} = 2.775(15)\,h^{-1} \times 10^{11} M_\odot/(h^{-1}\mathrm{Mpc})^3$ (Ast. parameters 2016; Planck Collaboration 2015-XIII); with the solar mass denoted by $M_\odot = 1.988 \times 10^{33}\mathrm{g}$ and h parameterises the present value of the Hubble parameter as

$$H_0 = 100h\,\mathrm{km\,s^{-1}Mpc^{-1}} = \frac{h}{3000}\mathrm{Mpc^{-1}}. \tag{8}$$

The latest value of the Hubble parameter obtained by the *Hubble Space Telescope* is quoted to be (Ligo colaboration 2017):

$$H_0 = 70.0^{12,0}_{-8,0}\,\mathrm{kms^{-1}Mpc^{-1}}. \tag{9}$$

It is usually more useful to measure the energy density as a fraction of the critical density, defining the *density parameter* $\Omega_i \equiv \rho_i/\rho_c$. The subscript i labels different constituents of the Universe, such as radiation or matter. The Friedmann equation (4) can then be written in such a way to relate the density parameter and the curvature of the Universe as

$$\Omega - 1 = \frac{k}{a^2H^2}. \tag{10}$$

Thus the correspondence between the total density content Ω and the space-time curvature for different k values is:

- Open Universe : $0 < \Omega < 1 :\ k < 0 :\ \rho < \rho_c$.
- Flat Universe : $\Omega = 1 :\ k = 0 :\ \rho = \rho_c$.
- Closed Universe: $\Omega > 1 :\ k > 0 :\ \rho > \rho_c$.

Current cosmological observations, based on the standard model, suggest the present value of Ω is (McCoy 2014)

$$\Omega_0 = 1.00 \pm 0.002, \tag{11}$$

that is, the present Universe is very nearly flat.

Shortcomings

Once we know what are the typical equations that describes the Universe, we need to know if the typical components in the cosmos (baryonic matter, radiattion, dark matter, etc) are enough to describes all the observations that we can see at this moment. In fact there are several "problems" that the standar old cosmology (without considering an inflationary period) can not explain. In this section we analize the most important of these problems. We introduce the concept of inflation and finally we show how this period can help us to solve this issues.

Flatness problem

We notice that $\Omega = 1$ is a special case of equation (10). If the Universe was perfectly flat at the earliest epochs, then it remained so for all time. Nevertheless a flat geometry is an unstable critical situation, that is, even a tiny deviation from it would cause that Ω evolved quite differently and very quickly the Universe would have become more curved. This can be seen as a consequence due to aH is a decreasing function of time during radiation or matter domination epoch. We observe this behaviour from (10):

$$\begin{aligned} \mid \Omega - 1 \mid \quad &\propto t \qquad \text{during radiation domination,} \\ \mid \Omega - 1 \mid \quad &\propto t^{2/3} \qquad \text{during dust domination.} \end{aligned}$$

Since the present age of the Universe is estimated to be $t_0 \simeq 13.80 \pm 0.04\,\text{Grs}$ (Ast. parameters 2016), from the above equation we can deduce the required value of $\mid \Omega - 1 \mid$ at different times in order to obtain the correct spatial-geometry at the present time. For instance, let us consider some particular epochs in a nearly flat universe,

- At Decoupling time ($t \simeq 10^{13}\,\text{sec}$), we need that $\mid \Omega - 1 \mid \leq 10^{-3}$.
- At Nucleosynthesis time ($t \simeq 1\,\text{sec}$), we need that $\mid \Omega - 1 \mid \leq 10^{-16}$.
- At the Planck epoch ($t \simeq 10^{-43}\,\text{sec}$), we need that $\mid \Omega - 1 \mid \leq 10^{-64}$.

Because there is no reason to prefer a Universe with critical density, hence $\mid \Omega - 1 \mid$ should not necessarily be exactly zero. Consequently, at early times $\mid \Omega - 1 \mid$ have to be fine-tuned extremely close to zero in order to reach its actual observed value.

Horizon problem

The horizon problem is one of the most important problems in the Big Bang model, as it refers to the communication between different regions of the Universe. Bearing in that mind, the *Anthropic Cosmological Principle* holds (Barrow & Tipler 1986; Coles & Lucchin 1995), which is intimately connected with the existence of the Big Bang, the age of the Universe is a finite quantity and hence even light should have only travelled a finite distance by any given time.

According the standard cosmology, photons decoupled from the rest of the components at temperatures about $T_{dec} \approx 0.3\,eV$ at redshift $z_{dec} \approx 1100$, from this time on photons free-streamed and travelled basically uninterrupted until reach us, giving rise to the region known as the Observable Universe. This spherical surface at which decoupling process occurred is called *surface of last scattering*. The primordial photons are responsible for the CMB observed today, then looking at its fluctuations is analogous of taking a picture of the universe at that time ($t_{dec} \approx 380,000$ yrs old), see Figure 1.

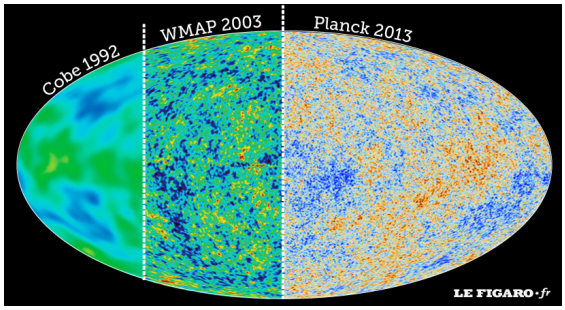

Fig. 1. Temperature fluctuations observed in the CMB using COBE-WMAP-Planck data ((Gold et al. 2011)(Planck Collaboration 2015-XI)(Planck Collaboration 2015-XVI)).

Figure 1 shows light seen in all directions of the sky, these photons randomly distributed have nearly the same temperature $T_0 = 2.725(7)$ K plus small fluctuations (about one part in one hundred thousand) (Ast. parameters (2016); **?**). As we have already pointed out, being at the same temperature is a property of thermal equilibrium. Observations are therefore easily explained if different regions of the sky had been able to interact and moved towards thermal equilibrium. In other words, the isotropy observed in the CMB might imply that the radiation was homogeneous and isotropic within regions located on the last scattering surface. Oddly, the comoving horizon over which causal interactions occurred before photons decoupled was significantly smaller than the comoving distance that radiation travelled after decoupling. This means that photons coming from regions of the sky separated by more than the horizon scale at last scattering, typically about 2°, would not had been able to interact and established thermal equilibrium before decoupling. A simple calculation displays that at decoupling time the comoving horizon was 90 h^{-1} Mpc (jav: checar) and would be stretched up to 2998 h^{-1} Mpc (jav: checar) at present time. Then, the microwave background should have consisted of about 10^5 causally disconnected regions (McCoy 2014). Therefore, the Big Bang model by itself does not offer an explanation on why temperatures seen in opposite sides of the sky are so accurately the same; the homogeneity must had been part of the initial conditions.

On the other hand, the microwave background is not perfectly isotropic, but instead exhibits small fluctuations as detected by, initially, the Cosmic Background Explorer satellite (COBE) (Smooth et al. 1992), then with improved measurements by the Wilkinson Microwave Anisotropy Probe (WMAP) (Hinshaw et al. 2009; Larson et al. 2011) and nowadays with the Planck satellite (Planck Collaboration 2016). These tiny irregularities are thought to be the 'seeds' that grew up until become the structure nowadays observed in the Universe.

Monopole problem

Following the line to find out the simplest theory to describe entirely the laws of the Universe, several models in particle physics were suggested to unified three of the four forces presented in the Standard Model of Particle Physics (SM): strong force, described by the group $SU(3)$, weak and electromagnetic force, with associated group $SU(2)\otimes U(1)$. These classes of theories are called *Grand Unified Theories (GUT)* (Georgi & Glashow 1974). An important point to mention in favour of GUT, is that they are the only theories that predict the equality electron-proton charge magnitude. Also, there are good reasons to believe that the origin of *baryon asymmetry* might have been generated by GUTs (Kolb & Turner 1983).

Basically, these kind of theories assert that in the early stages of the Universe ($t \sim 10^{-43}\,\mathrm{sec}$), at highly extreme temperatures ($T_{GUT} \sim 10^{32}\,\mathrm{K}$), existed a unified or *symmetric phase* described by a group G. As the Universe temperature dropped off, it went through many different phase transitions until reach the matter particles such as electrons, protons, neutrons, photons. When a phase transition happens, its symmetry is broken, thus the symmetry group changes by itself. For instance:

- GUT transition:

$$G \to SU(3) \otimes SU(2) \otimes U(1).$$

- Electroweak transition:

$$SU(3) \otimes SU(2) \otimes U(1) \to SU(3) \otimes U(1).$$

The phase transitions have plenty of implications. One of the most important is the *topological defects* production which depends on the type of symmetry breaking and the spatial dimension (Vilenkin & Shellard 2000), some of them are:

- Monopoles (zero dimensional).
- Strings (one dimensional).
- Domain Walls (two dimensional).
- Textures (three dimensional).

Monopoles are therefore expected to emerge as a consequence of unification models. Besides that, from particle physics models, there are not theoretical constraints on the mass a monopole should carry. However, from LHC constrictions and grand unification theories, the mass of the monopole could be $4\times10^3-10^{16}$ GeV (Mermod 2013). Hence, based on their non-relativitic character, a crude calculation predicts an extremely high abundance at present time (Coles & Lucchin 1995)

$$\Omega_M \simeq 10^{16}.$$

According to this prediction, the Universe would be dominated by magnetic monopoles, in contrast with current observations: no one has found anyone (Ambrosio 2002).

3. COSMOLOGICAL INFLATION

The inflationary model offers the most elegant way so far proposed to solve the problems of the standard big bang and therefore to understand why the universe is so remarkably in agreement with the standard cosmology. It does not replace the Big Bang model, but rather it is considered as an 'auxiliary patch' which occurred at the earliest stages without disturbing any of its successes.

Inflation is defined as the epoch in the evolution of the Universe in which the scale factor is quickly accelerated in just a fraction of a second:

$$\text{INFLATION} \iff \ddot{a} > 0 \tag{12}$$

$$\iff \frac{d}{dt}\left(\frac{1}{aH}\right) < 0. \tag{13}$$

The last term corresponds to the comoving Hubble length $1/(aH)$ which is interpreted as the observable Universe becoming smaller during inflation. This process allows our observable region to lay within a region that was inside the Hubble radius at the beginning of inflation, in Liddle (1999) words "is something similar to zooming in on a small region of the initial universe", see Figure 2.

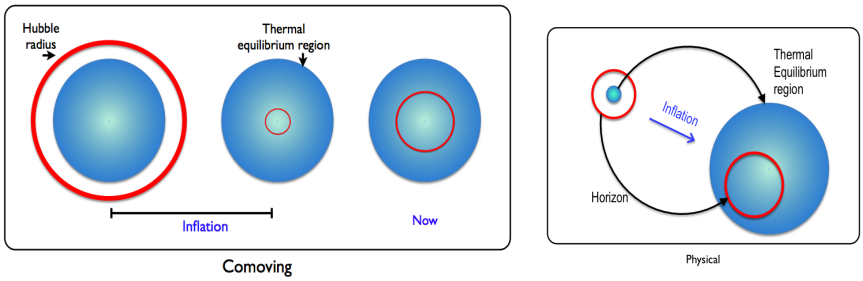

Fig. 2. Left: Schematic behaviour of the comoving Hubble radius during the inflationary period. Right: Physical evolution of the observable universe during the inflationary period.

From the acceleration equation (5) the condition for inflation, in terms of the material required to drive the expansion, is

$$\ddot{a} > 0 \Longleftrightarrow (\rho + 3p) < 0. \tag{14}$$

Because in standard physics it is always postulated ρ as a positive quantity, and then to satisfy the acceleration condition is necessary for the overall pressure to have

$$\text{INFLATION} \iff p < -\rho/3. \tag{15}$$

Nonetheless, neither a radiation nor a matter component satisfies such condition. Let us postpone for a bit the problem of finding a 'candidate' which may satisfy this inflationary condition.

3.1. *Solution of the Big Bang Problems*

If this brief period of accelerated expansion occurred, then it is possible that the aforementioned problems of the Big Bang could be solved.

Flatness problem

A typical solution is a universe possessing a cosmological constant Λ, which can be interpreted as a perfect fluid with equation of state $p = -\rho$. Having this condition, since H is constant, we observe from the Friedmann equation (4) that the universe is exponentially expanded:

$$a(t) \propto \exp(Ht), \tag{16}$$

then, the condition (13) is naturally fulfilled. This epoch is called *de Sitter stage*. However, postulating a cosmological constant might create more problems than solutions by itself (Carroll 2001).

Let us look what happens when a general solution is considered. If somehow there was an accelerated expansion, $1/(aH)$ tends to be smaller on time and hence, by the expression (10), Ω is driven towards the unity rather than away from it. Then, we may ask ourselves by how much should $1/(aH)$ decrease. If the inflationary period started at time $t = t_i$ and ended up approximately at the beginning of the radiation dominated era ($t = t_f$), then

$$\mid \Omega - 1 \mid_{t=t_f} \sim 10^{-60},$$

and

$$\frac{\mid \Omega - 1 \mid_{t=t_f}}{\mid \Omega - 1 \mid_{t=t_i}} = \left(\frac{a_i}{a_f}\right)^2 \equiv e^{-2N}. \tag{17}$$

So, the required condition to reproduce the value of Ω_0 =? (jav: valor) today is that inflation lasted for at least $N \equiv \ln a \gtrsim 60$, then Ω will be extraordinarily close to one that we still observe it today. In this sense, inflation

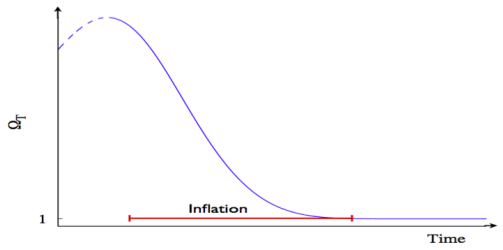

Fig. 3. Evolution of the density parameter Ω , during the inflationary period. Ω is driven towards unity, rather than away from it.

magnifies the curvature radius of the universe, so locally the universe seems to be flat with great precision, Figure 3.

Horizon problem

As we have already seen, during inflation the universe expands drastically and there is a reduction in the comoving Hubble length. This allowed a tiny region located inside the Hubble radius to evolve and constitute our present observable Universe. Fluctuations were hence stretched outside of the horizon during inflation and re-entered the horizon in the late Universe, see Figure 2. Scales that were outside the horizon at CMB decoupling were in fact inside the horizon before inflation. The region of space corresponding to the observable universe therefore was in thermal equilibrium before inflation and the uniformity of the CMB is essentially explained.

Monopole problem

The monopole problem was initially the motivation to develop the inflationary cosmology (Guth 1997). During the inflationary epoch, the Universe led to a dramatic expansion over which the density of the unwanted particles were diluted away. Generating enough expansion, the dilution made sure the particles stayed completely out of the observable Universe making pretty difficult to localise even a single monopole.

4. SINGLE-FIELD INFLATION

Throughout the literature there exists a broad diversity of models that have been proposed for inflation (Liddle & Lyth 2000; Olive 1990; Lyth & Riotto 1999). In this section we present the scalar fields as good candidates to drive inflation and explain how relate theoretical predictions to observable quantities. Here, we limit ourselves to models based on general gravity, i.e. derived from the Einstein-Hilbert action, and single-field models described by

a homogeneous slow-roll scalar field ϕ.

Inflation relies on the existence of an early epoch in the universe dominated by a very different form of energy; remember the requirement of the unusual property of a negative pressure. Such condition can be satisfied by a simple scalar field (spin-0 particle). The scalar field which drives the Universe to an inflationary epoch is often termed as the *inflaton field*.

Let us consider a scalar field minimally coupled to gravity, with an arbitrary potential $V(\phi)$ and Lagrangian density $\mathcal{L}$ specified by

$$S = \int d^4x \sqrt{-g}\, \mathcal{L} = \int d^4x \sqrt{-g} \left[\frac{1}{2}\partial_\mu\phi\partial^\mu\phi - V(\phi)\right]. \tag{18}$$

The energy-momentum tensor corresponding to this scalar field Lagrangian is given by

$$T_{\mu\nu} = \partial_\mu\phi\partial_\nu\phi - g_{\mu\nu}\,\mathcal{L}. \tag{19}$$

In the same way as the perfect fluid treatment, the energy density ρ_ϕ and pressure density p_ϕ in FRW metric are found to be

$$T_{00} = \rho_\phi = \frac{1}{2}\dot{\phi}^2 + V(\phi) + \frac{(\nabla\phi)^2}{2a^2}, \tag{20}$$

$$T_{ii} = p_\phi = \frac{1}{2}\dot{\phi}^2 - V(\phi) - \frac{(\nabla\phi)^2}{6a^2}. \tag{21}$$

Considering a homogeneous field, its equation of state corresponding is

$$w = \frac{P}{\rho} = \frac{\frac{1}{2}\dot{\phi}^2 - V(\phi)}{\frac{1}{2}\dot{\phi}^2 + V(\phi)}. \tag{22}$$

We can now split the inflaton field as

$$\phi(\mathbf{x}, t) = \phi_0(t) + \delta\phi(\mathbf{x}, t), \tag{23}$$

where ϕ_0 is considered a classical field, that is, the mean value of the inflaton on the homogeneous and isotropic state, whereas $\delta\phi(\mathbf{x}, t)$ describes the quantum fluctuations around ϕ_0.
The evolution equation for the background field ϕ_0 is given by

$$\ddot{\phi_0} + 3H\dot{\phi_0} = -V'(\phi_0), \tag{24}$$

and moreover, the Friedmann equation (4) with negligible curvature becomes

$$H^2 = \frac{8\pi}{3m_{Pl}^2}\left[\frac{1}{2}\dot{\phi}_0^2 + V(\phi_0)\right], \tag{25}$$

where we have used primes as derivatives with respect to the scalar field ϕ_0.

From the structure of the effective energy density and pressure, the acceleration equation (5) becomes,

$$\frac{\ddot{a}}{a} = -\frac{8\pi}{m_{Pl}^2}\left(\dot{\phi}_0^2 - V(\phi_0)\right). \tag{26}$$

Therefore, the inflationary condition to be satisfied is $\dot{\phi}_0^2 < V(\phi_0)$, and it is easily fulfilled with a suitably flat potential. Now on we will omit the subscript '0' by convenience.

4.1. *Slow-roll approximation*

As we have noted, a period of accelerated expansion can be created by the cosmological constant (Λ) and hence solve the aforementioned problems. After a brief period of time, inflation must end up and its energy being converted into conventional matter/radiation, this process is called *reheating*. In a Universe dominated by a cosmological constant the reheating process is seen as Λ decaying into conventional particles, however claiming that Λ is able to decay is still a naive way to face the problem. On the other hand, scalar fields have the property to behave like a *dynamical cosmological constant*. Based on this approach, it is useful to suggest a scalar field model starting with a nearly flat potential, i.e. initially satisfies the *first slow-roll* condition $\dot{\phi}^2 \ll V(\phi)$. This condition may not necessarily be fulfilled for a long time. To avoid this problem, the second *slow-roll* condition is defined as $|\ddot{\phi}| \ll |V_{,\phi}|$ or equivalently $|\ddot{\phi}| \ll 3H|\dot{\phi}|$. In this case the scalar field is slowly rolling down its potential and by obvious reasons such approximation is called *slow-roll* (Liddle & Lyth 1992; Liddle et al. 1994). The equations of motion (24) and (25), for slow-roll inflation, then become

$$3H\dot{\phi} \simeq -V'(\phi), \tag{27}$$

$$H^2 \simeq \frac{8\pi}{3m_{Pl}^2}V(\phi). \tag{28}$$

It is easily verifiable that the slow-roll approximation requires the slope and curvature of the potential to be small: $V', V'' \ll V$.

The inflationary process can be summarised as an accelerated Universe which takes place when the kinetic part of the inflaton field is subdominant over the potential field $V(\phi)$ term. Then, when both quantities become comparable the inflationary period ends up given rise finally to the reheating process, see Fig. 4.

It is now useful to introduce the potential slow-roll parameters $\epsilon_{\rm v}$ and $\eta_{\rm v}$ in the following way (Liddle & Lyth 1992)

$$\epsilon_{\rm v}(\phi) \equiv \frac{m_{Pl}^2}{16\pi}\left(\frac{V'(\phi)}{V(\phi)}\right)^2, \tag{29}$$

$$\eta_{\rm v}(\phi) \equiv \frac{m_{Pl}^2}{8\pi}\frac{V''(\phi)}{V(\phi)}. \tag{30}$$

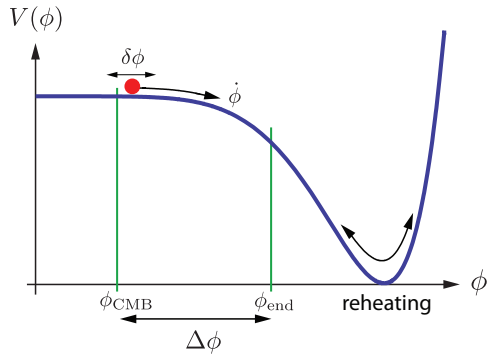

Fig. 4. Schematic inflationary process (Baumann & Peiris 2009).

Equations (27) and (28) are in agreement with the slow-roll approximation when the following conditions hold

$$\epsilon_{\rm v}(\phi) \ll 1, \quad |\,\eta_{\rm v}(\phi)\,| \ll 1.$$

These conditions are sufficient but not necessary, because the validity of the slow-roll approximations was a requirement in its derivation. The physical meaning of $\epsilon_{\rm v}(\phi)$ can be explicitly seen by expressing equation (12) in terms of ϕ, then, the inflationary condition is equivalent to

$$\frac{\ddot{a}}{a} > 0 \implies \epsilon_{\rm v}(\phi) < 1. \tag{31}$$

Hence, inflation concludes when the value $\epsilon_{\rm v}(\phi_{end}) = 1$ is approached.

Within these approximations, it is straightforward to find out the scale factor a between the beginning and the end of inflation. Because the size of the expansion is an enormous quantity, it is useful to compute it in terms of the e-fold number N defined by

$$N \equiv \ln \frac{a(t_{end})}{a(t)} = \int_t^{t_e} H\, dt \simeq \frac{8\pi}{m_{Pl}^2} \int_{\phi_e}^{\phi} \frac{V}{V'} d\phi. \tag{32}$$

To give an estimate of the number of e-folds N, let us consider that the evolution of the Universe can be split up into different epochs:

- Inflationary era: horizon crossing ($k = aH$) $\rightarrow$ end of inflation a_{end}.
- Radiation era: reheating $\rightarrow$ matter-radiation equality a_{eq}.
- Matter era: $a_{eq} \rightarrow$ present a_0.

Assuming the transition between one era to another is instantaneous, then $N(k) = \ln(a_k/a_0)$ can be easily computed with:

$$\frac{k}{a_0 H_0} = \frac{a_k H_k}{a_0 H_0} = \frac{a_k}{a_{end}} \frac{a_{end}}{a_{reh}} \frac{a_{reh}}{a_{eq}} \frac{a_{eq}}{a_0} \frac{H_k}{H_0}.$$

Then, one has (Liddle & Lyth 2000)

$$N(k) = 62 - \ln\frac{k}{a_0 H_0} - \ln\frac{10^{16} GeV}{V_k^{1/4}} + \ln\frac{V_k^{1/4}}{V_{end}} - \frac{1}{3}\ln\frac{V_{end}^{1/4}}{\rho_{reh}^{1/4}}.$$

The last three terms are small quantities related with energy scales during the inflationary process and usually can be ignored. The precise value for the second quantity depends on the model as well as the COBE normalisation, however it does not present any significant change to the total amount of e-folds. Thus, the value of total e-foldings is ranged from 50-70 (Lyth & Riotto 1999). This value could change if a modification of the full history of the Universe is considered. For instance, thermal inflation can alter N up to a minimum value of N=25 (Lyth & Stewart 1995, 1996a).

As we noted, the parameters to describe inflation can be presented as a function of the scalar field potential. That is, specifying an inflationary model with a single scalar field is just selecting an inflationary potential $V(\phi)$. At this point, it is necessary to mention that these inflationary potentials are not chosen arbitrarily. In fact, there is a whole line of research in models of particle physics that are looking for inflationary potentials motivated by fundamental physics. However, for the purposes of this paper, we will not delve into this subject. In this way, every time we mention that we are taking an inflationary potential, it will be understood that this potential is motivated by a fundamental theory. In order to exemplify our point, let us consider the following example.

The potential which describes a massive scalar field is given by:

$$V(\phi) = \frac{1}{2}m^2\phi^2. \tag{33}$$

Considering the slow-roll approximation, equations (24) and (25) become:

$$\begin{aligned} 3H\dot{\phi} &= -m^2\phi, \\ H^2 &= \frac{4\pi m^2\phi^2}{3m_{pl}^2}. \end{aligned} \tag{34}$$

Thus, the dynamics of this type of model is described by

$$\begin{aligned} \phi(t) &= \phi_i - \frac{m m_{pl}}{\sqrt{12\pi}}\, t, \\ a(t) &= a_i \exp\left[\sqrt{\frac{4\pi}{3}}\frac{m}{m_{pl}}\left(\phi_i t - \frac{m m_{pl}}{\sqrt{48\pi}}t^2\right)\right], \end{aligned} \tag{35}$$

where ϕ_i and a_i represent the initial conditions at a given initial time $t = t_i$. The slow-roll parameters for this particular potential are computed from equations (29) and (30)

$$\epsilon_{\rm v} = \eta_{\rm v} = \frac{m_{pl}^2}{4\pi}\frac{1}{\phi^2}, \tag{36}$$

that is, an inflationary epoch takes place whilst the condition $|\phi| > m_{pl}/\sqrt{4\pi}$ is satisfied, and the total amount lapse during this accelerated period is encoded on the e-folds number

$$N_{tot} = \frac{2\pi}{m_{pl}^2}\left[\phi_i^2 - \phi_e^2\right]. \tag{37}$$

The steps shown before might, in principle, apply to any inflationary single-field model. That is, the general information we need to characterised cosmological inflation is specified by its potential.

4.2. *Cosmological Perturbations*

Inflationary models have the merit that they do not only explain the homogeneity of the universe on large-scales, but also provide a theory for explaining the observed level of *anisotropy*. During the inflationary period, quantum fluctuations of the field were driven to scales much larger than the Hubble horizon. Then in this process, the fluctuations were frozen and turned into metric perturbations (Mukhanov & Chibisov 1997). Metric perturbations created during inflation can be described in terms of two types of perturbations. The *scalar, or curvature,* perturbations are coupled with matter in the universe and form the initial "seeds" of structure formation. On the other hand, although the *tensor perturbations* do not couple to matter, they are associated to the generation of gravitational waves. As we shall see, scalar and tensor perturbations are seen as the important components to the CMB anisotropy (Hu & Dodelson 2002).

In the same way we have introduced the density parameter for large scales, on small scales we consider the *density contrast* defined by $\delta \equiv \delta\rho/\rho$. We now on assume that the density contrast for different species in the Universe satisfies the *adiabatic conditions*

$$\frac{1}{3}\delta_{\mathbf{k}b} = \frac{1}{3}\delta_{\mathbf{k}c} = \frac{1}{4}\delta_{\mathbf{k}\gamma}\left(= \frac{1}{4}\delta_{\mathbf{k}}\right). \tag{38}$$

The most general perturbation on the density is described by a linear combination between adiabatic perturbation as well as *isocurvature perturbation*, which the latter one plays and important role when more than one scalar field is considered (Liddle & Lyth 2000).

We introduce the *primordial curvature perturbation* $\mathcal{R}_k(t)$, which has the property to be constant within few Hubble times after the horizon exit given by $k = aH$. This constant value is called the *primordial value* and is related with the scalar field perturbation $\delta\phi$ by

$$\mathcal{R}_k = -\left[\frac{H}{\dot{\phi}}\ \delta\phi_k\right]_{k=aH}. \tag{39}$$

Then, the primordial curvature power spectrum $\mathcal{P}_{\mathcal{R}}(k)$ is computed from

$$\mathcal{P}_{\mathcal{R}}(k) = \left[\left(\frac{H}{\dot{\phi}}\right)^2 \mathcal{P}_{\phi}(k)\right]_{k=aH}. \tag{40}$$

As it was explained before, if we consider that inflation is at least exponential, then the horizon remains practically constant while all other scales grow. In this way, we can focus on the evolution of the quantum perturbations of the inflaton in a small region compared to the horizon. In this region it is possible to consider the space as locally flat and ignore the metric perturbations. Thus, working in the fourier space, the classical equation of motion of the perturbation part of $\phi(\mathbf{x}, t)$ in (23) is

$$(\delta\phi_k)^{\cdot\cdot} + 3H(\delta\phi_k)^{\cdot} + \left(\frac{k}{a}\right)^2 \delta\phi_k = 0, \tag{41}$$

where we have assumed $\delta\phi$ is linear. This basically means that perturbations generated by vacuum fluctuations have uncorrelated Fourier modes, the signature of *Gaussian perturbations*.

The above equation can be rewritten as the equation of a harmonic oscillator with a variable frequency. If we now move to the quantum world and make the corresponding associations of operators to each classical variable, the quantum dynamics will be determined by (for a detailed explanation see (Liddle & Lyth 2009), page 382)

$$\hat{\psi}_k(\eta) = \frac{\psi_k(\eta)\,\hat{a}(k) + \psi_k^*((\eta)\,\hat{a}^\dagger(-k)}{(2\pi)^3} \quad \text{with} \quad \psi_k(\eta) = -\frac{e^{-ik\eta}}{\sqrt{2k}}\frac{k\eta - i}{k\eta}, \tag{42}$$

where $\hat{a}$ and $\hat{a}^\dagger$ are the particle creation and annihilation operators, η is the proper time defined by $\eta \equiv -1/aH$ and $\psi \equiv a\delta\phi$.

The inflationary process dilutes all possible particles existing before this period. Taking into account this, it is considered that the state in which the system is located is that of the vacuum. Defining the spectrum of perturbations as $\langle\psi_k\psi_k\rangle = 2\pi^2\mathcal{P}_\psi(k)\,\delta^3\left(\vec{k} + \vec{k}'\right)$ and evaluating it a few hubble times after the horizon exit, $\eta = 1/aH_k$, with H_k the value of the hubble constant at the time the scale k has left the horizon, it can be shown that the spectrum is given by

$$\mathcal{P}_\phi(k) = \left(\frac{H}{2\pi}\right)^2_{k=aH}, \tag{43}$$

and from (43) and (40) the spectrum of the curvature perturbation is

$$\mathcal{P}_\mathcal{R}(k) = \left[\left(\frac{H}{\dot{\phi}}\right)\left(\frac{H}{2\pi}\right)\right]^2_{k=aH}. \tag{44}$$

We notice that well after horizon exit, $\eta \to 0$, $\psi_k(\eta)$ approaches to

$$\psi_k(\eta) = -\frac{i}{\sqrt{2k}}\frac{1}{k\eta}, \tag{45}$$

so that equation 42 is rewritten as

$$\hat{\psi}_k(t) = \psi_k(t)\,\frac{\hat{a}(k) - \hat{a}^\dagger(-k)}{(2\pi)^3}. \tag{46}$$

In this way, it can be seen that the temporal dependence of $\hat{\psi}_k$ is now tribial. It implies that once $\psi_k(t)$ is messured in a time well after horizon exit, it will continue having a definite value. In this way, we can consider that this quantum fluctuation has become classical once it has crossed the horizon and therefore, the spectrum of quantum perturbations can be taken as the Initial inhomogeneities that will later give rise to the formation of structure. However, as will be seen below, these initial conditions will be slightly modified due to the amount of inflation remaining, once the k-scale has left the horizon.

On the other hand, the creation of gravitational waves corresponds to the tensor part of the metric perturbation $h_{\mu\nu}$ in (2). In Fourier space, tensor perturbations h_{ij} can be expressed as the superposition of two polarisation modes

$$h_{ij} = h_+ e_{ij}^+ + h_\times e_{ij}^\times, \tag{47}$$

where $+$, $\times$ represent the longitudinal and transverse modes. From Einstein equations it is found that each amplitude h_+ and $h_\times$ behaves as a free scalar field in the sense that

$$\psi_{+,\times} \equiv \frac{m_{Pl}}{\sqrt{8}}\, h_{+,\times}. \tag{48}$$

Therefore, taking the results of the scalar perturbations, each $h_{+,\times}$ has a spectrum $\mathcal{P}_T$ given by

$$\mathcal{P}_T(k) = \frac{8}{m_{Pl}^2}\left(\frac{H}{2\pi}\right)^2_{k=aH}. \tag{49}$$

The canonical normalisation of the field $\psi_{+,\times}$ was chosen such that the *tensor-to-scalar ratio* of the spectra is

$$r \equiv \frac{\mathcal{P}_T}{\mathcal{P}_\mathcal{R}} = 16\epsilon. \tag{50}$$

During the horizon exit epoch $k = aH$, H and $\dot{\phi}$ have tiny variations during few Hubble times. In this case, the scalar and tensor spectra are nearly scale invariant and therefore well approximated by power laws

$$\mathcal{P}_\mathcal{R}(k) = \mathcal{P}_\mathcal{R}(k_0)\left(\frac{k}{k_0}\right)^{n_\mathrm{s}-1}, \qquad \mathcal{P}_T(k) = \mathcal{P}_T(k_0)\left(\frac{k}{k_0}\right)^{n_T}. \tag{51}$$

where the spectral indices are defined as

$$n_\mathrm{s} - 1 \equiv \frac{d\ln\mathcal{P}_\mathcal{R}(k)}{d\ln k}, \qquad n_T \equiv \frac{d\ln\mathcal{P}_T(k)}{d\ln k}. \tag{52}$$

A scale-invariant spectrum, called Harrison-Zel'dovich (HZ), has constant variance on all length scales and it is characterised by $n_\mathrm{s} = 1$: small deviations from scale-invariance are also considered as a typical signature of the inflationary models. Then the spectral indices n_s and n_T can be expressed in terms of the slow-roll parameters ϵ_v and η_v, to lowest order, as:

$$\begin{aligned} n_{\rm s} - 1 &\simeq -6\,\epsilon_{\rm v}(\phi) + 2\,\eta_{\rm v}(\phi), \\ n_T &\simeq -2\,\epsilon_{\rm v}(\phi). \end{aligned} \tag{53}$$

The parameters are *not* completely independent each other, but the tensor spectral index is proportional to the tensor-to-scalar ratio $r = -8n_T$. This expression is considered as the *first consistency relation* for slow-roll inflation. Hence, any inflationary model, to the lowest order in slow-roll, can be described in terms of three independent parameters: the amplitude of density perturbations $\delta_H \equiv 2/5 P_{\mathcal{R}}^{1/2} \approx 2 \times 10^{-5}$, the scalar spectral index $n_{\rm s}$, and the tensor-to-scalar ratio r. In case we need a more accurate description we have to consider higher-order effects, and then include parameters for describing the running of scalar ($n_{s_{run}} \equiv dn_{\rm s}/d\ln k$) and tensor ($n_{T_{run}} \equiv dn_T/d\ln k$) index and higher order corrections.

An important point to emphasise is that δ_H, r and $n_{\rm s}$ are *observable* parameters that nowadays are tested from several experiments. This allows us to compare theoretical predictions with observational data, for instance, those provided by the Cosmic Microwave Background radiation. In other words, future measurements of these parameters may probe or at least constrain the inflationary models and therefore the shape of the inflaton potential $V(\phi)$.

Let us get back to the massive scalar field example in equation (33): Inflation ends up when the condition $\epsilon_{\rm v} = 1$ is achieved, so $\phi_{end} \simeq m_{pl}/\sqrt{4\pi}$. As we pointed out before, we are interested in models with an e-fold number of about $N_{tot} = 60$, that is

$$\phi_i = \phi_{60} \simeq \sqrt{\frac{30}{\pi}} m_{pl}. \tag{54}$$

Finally, the spectral index and the tensor-to-scalar ratio for this potential are

$$n_{\rm s} - 1 = -\frac{m_{pl}^2}{\pi \phi_{60}^2}, \qquad r = \frac{m_{pl}^2}{\phi_{60}^2}. \tag{55}$$

If the massive scalar field potential is the right inflationary model, current observations should favour the values $n_s \approx 0.97$ and $r \approx 0.1$.

5. INFLATIONARY MODELS

We have seen that an inflationary model is described by the specification of the potential form $V(\phi)$ relevant during inflation. Then, the comparison of model predictions to CMB observations reduces to the following basic steps:

1. Given a scalar field potential $V(\phi)$, compute the slow roll parameters $\epsilon_{\rm v}(\phi)$ and $\eta_{\rm v}(\phi)$.

2. Find out ϕ_{end} by $\epsilon(\phi_{end}) = 1$.

3. From (32), compute the field ϕ_{60}.

4. Compute $n_{\rm s}$ and r as functions of ϕ, and finally evaluate them at $\phi = \phi_{60}$ which can be tested by CMB temperature anisotropy data.

Different types of models are classified by the relation among their slow-roll parameters ϵ and η, which can be reflected on different relations between $n_{\rm s}$ and r. Hence, an appropriate parameter space to show the diversity of models is well described by the $n_{\rm s}$—r plane.

5.1. *Models*

Even if we restrict the analysis to a simple single-field, the number of inflationary models available is enormous (Liddle & Lyth 2000; Lyth & Riotto 1999; Linde 2005). Then, it is convenient to classify different kinds of scalar field potentials following (Kinney 2004). The classification is based on the behaviour of the scalar field potential during inflation. The three basic types are shown in Figure 5. *Large field*: the field is initially displaced from a stable minimum and evolves towards it. *Small field*: the field evolves away from an unstable maximum. *Hybrid*: the field evolves towards a minimum with vacuum energy different to zero.

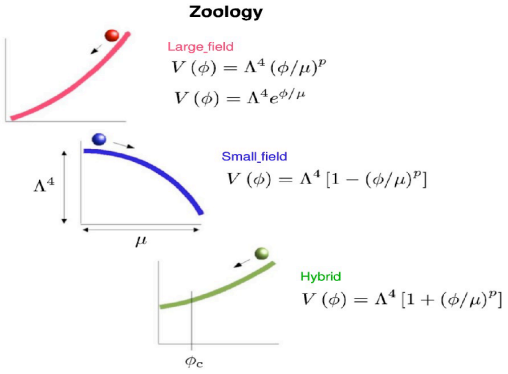

Fig. 5. Potential classification. From top to bottom: *large field, small field and hybrid potential* (Kinney 2004).

A general single field potential can be written in terms of a *height* Λ and a *width* μ as

$$V(\phi) = \Lambda^4 f\left(\frac{\phi}{\mu}\right). \tag{56}$$

Different models have different forms for the function f.

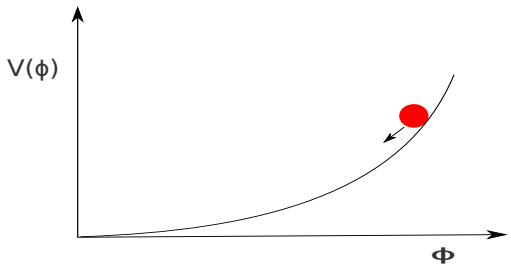

Fig. 6. Chaotic inflationary potential.

5.2. *Large-field models:* $-\epsilon < \eta \leq \epsilon$

Large field models perhaps posses the simplest type of monomial potentials. These kind of potentials represent the *chaotic* inflationary scenarios (Linde 1983). The distinctive of these models is that the shape of the effective potential is not very important in detail. That is, a region of the Universe where the scalar field is usually situated at $\phi \sim m_{\rm Pl}$ from the minimum of its potential will automatically lead to inflation, see Figure 6. Such models are described by $V''(\phi) > 0$ and $-\epsilon < \eta \leq \epsilon$.

A general set of large-field polynomial potentials can be written as

$$V(\phi) = \Lambda^4 \left(\frac{\phi}{\mu}\right)^p , \tag{57}$$

where it is enough to choose the exponent $p > 1$ in order to specify a particular model. This model gives

$$\begin{aligned} n_{\rm s} - 1 &= -\frac{2+p}{2N} , \\ r &= \frac{4p}{N} . \end{aligned} \tag{58}$$

In this case, gravitational waves can be sufficiently big to eventually be observed ($r \gtrsim 0.1$).

From the quadratic potential of equation (33), we obtain

$$\epsilon \simeq 0.008, \quad \eta \simeq 0.008, \quad n_{\rm s} \simeq 0.97, \quad r \simeq 0.128 \tag{59}$$

In the high power limit the $V \propto \phi^p$ predictions are the same as the exponential potential (La & Steinhardt 1999). Hence, a variant of this class of models is

$$V(\phi) = \Lambda^4 \exp(\phi/\mu) . \tag{60}$$

This type of potential is a rare case presented in inflation, that is because its dynamics has an exact solution given by a power-law expansion. For this case the spectral index $n_{\rm s}$ is closely related to the tensor-to-scalar ratio r, as

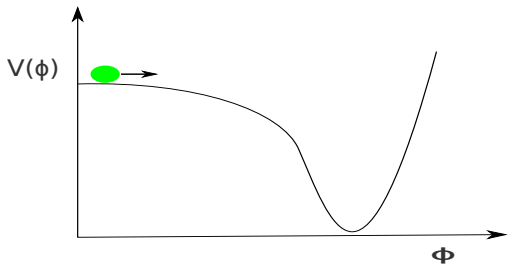

Fig. 7. New inflationary potential.

$$\begin{aligned} n_{\rm s} - 1 &= -\frac{m_{pl}^2}{8\pi\mu^2}, \\ r &= 8\left(1 - n_{\rm s}\right), \end{aligned} \tag{61}$$

as we observe, the slow-roll parameters are explicitly independent of the e-fold number N.

5.3. *Small-field models:* $\eta < -\epsilon$

Small field models are typically described by potentials which arise naturally from spontaneous symmetry breaking, these type of models are also known as *new inflation* (Albrecht & Steinhardt 1982; Linde 1983). In this case, inflation takes place when the field is situated in a false vacuum state, very close to the top of the hill and rolls down to a stable minimum, see Figure 7. These models are typically characterized by $V''(\phi) < 0$ and $\eta < -\epsilon$, usually ϵ (and hence the tensor amplitude) is closely zero.
Small field potentials, can be written in the generic form as

$$V(\phi) = \Lambda^4 \left[1 - (\phi/\mu)^p\right], \tag{62}$$

where the exponent p differs from model to model. $V(\phi)$ is usualy considered as the lowest-order in a Taylor expansion from a more general potential. In the simplest case of spontaneous symmetry breaking with no special symmetries, the dominant term is the mass term, $p = 2$, hence the model gives

$$\begin{aligned} n_{\rm s} - 1 &\simeq -4\left(\frac{m_{\rm Pl}}{\mu}\right)^2, \\ r &= 8(1 - n_{\rm s}) \exp\left[-1 - N\left(1 - n_s\right)\right]. \end{aligned} \tag{63}$$

On the other hand, $p > 2$ has a very different behavior. The scalar spectral index is

$$n_{\rm s} - 1 = -\frac{2}{N}\left(\frac{p-1}{p-2}\right), \tag{64}$$

independent of $(m_{\rm Pl}/\mu)$. In addition, when $\mu < m_{\rm Pl}$ the values of r are restricted by

$$r < 8\frac{p}{N\,(p-2)}\left[\frac{8\pi}{Np\,(p-2)}\right]^{p/(p-2)}. \tag{65}$$

5.4. *Hybrid models:* $0 < \epsilon < \eta$

The third class called **hybrid** frequently includes models which incorporate supersymmetry into inflation (Linde 1991; Copeland et al. 1994). In these models, the inflaton field ϕ evolves towards a minimum of its potential, however, the minimum has a vacuum energy $V(\phi_{\rm min}) = \Lambda^4$ which is different to zero. In such cases, inflation continues forever unless an auxiliary field ψ is added to interact with ϕ and ends inflation at some point $\phi = \phi_{\rm c}$. Such models are well described by $V''\,(\phi) > 0$ and $0 < \epsilon < \eta$.

The generic potential for hybrid inflation, in a similar way to large field and small field models are considered, is

$$V\,(\phi) = \Lambda^4\left[1 + (\phi/\mu)^p\right]. \tag{66}$$

For $(\phi_N/\mu) \gg 1$ the behaviour of the large-field models is recovered. Besides that, when $(\phi_N/\mu) \ll 1$ the dynamics is similar to small-field models, but now the field is evolving towards a dynamical fixed point rather than away from it. Because the presence of an auxiliary field the number of e-folds is

$$N(\phi) \simeq \left(\frac{p+1}{p+2}\right)\left[\frac{1}{\eta(\phi_c)} - \frac{1}{\eta(\phi)}\right]. \tag{67}$$

For $\phi \gg \phi_c$, $N(\phi)$ approaches the value

$$N_{max} \equiv \left(\frac{p+1}{p+2}\right)\frac{1}{\eta(\phi_c)}, \tag{68}$$

and therefore, the spectral index is given by

$$n_{\rm s} - 1 \simeq 2\left(\frac{p+1}{p+2}\right)\frac{1}{N_{max} - N}.$$

As we can note, the power spectrum is *blue* ($n_{\rm s} > 1$) and besides that, the model presents a running of the spectral index

$$\frac{dn_{\rm s}}{d\ln k} = -\frac{1}{2}\left(\frac{p+2}{p+1}\right)(n_{\rm s} - 1)^2. \tag{69}$$

This parameter will be very useful for higher orders and more accurate constraints in future observations. For instance, if it is considered the particular case with $p = 2$ and $n_{\rm s} = 1.2$, the running obtained is $dn_{\rm s}/d\ln k = -0.05$ (Kinney & Riotto 1998).

5.5. *Linear models:* $\eta = -\epsilon$

Linear models, $V(\phi) \propto \phi$, are located on the limit between large field and small field models. They are represented by $V''(\phi) = 0$ and $\eta = -\epsilon$. The spectral index and tensor-to-scalar ratio are given by

$$n_{\rm s} - 1 = -\frac{6}{4N+1}, \qquad r = \frac{16}{4N+1}. \tag{70}$$

5.6. *Other single models*

There still remain several single-field models which cannot fit into this classification, for instance the logarithmic potentials (Barrow & Parsons 1995)

$$V(\phi) = V_0 \left[1 + (Cg^2/8\pi^2) \ln(\phi/\mu)\right]. \tag{71}$$

Typically they correspond to loop corrections in a supersymmetric theory, where C denotes the degrees of freedom coupled to the inflaton and g is a coupling constant. For this potential, the inflationary parameters are

$$\begin{aligned} n_{\rm s} - 1 &\simeq -\frac{1}{N}\left(1 + \frac{3Cg^2}{16\pi^2}\right), \\ r &\simeq \frac{1}{N}\frac{Cg^2}{4\pi}. \end{aligned} \tag{72}$$

In this model, to end up inflation, an auxiliary field is needed, which is the main feature of hybrid models. However when it is plotted on the $n_{\rm s}$—r plane, is located into the small-field region.

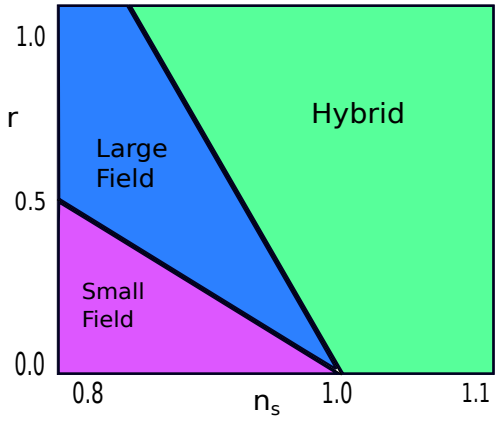

Fig. 8. Classification of the potentials in terms of $n_{\rm s}$ and r parameters.

The classification of inflationary models mentioned previously may be interpreted as an arbitrary one. Although, it is very useful because different types of models cover different regions of the $(n_{\rm s}, r)$ plane without overlaping, see Figure 8.

5.7. *Multi-field models*

There are some jobs where it is considered that there is more than one scalar field responsible for generating inflation in the early universe. However, because we are interested just in the last 50-60 e-folds, it is spected that no more than 2 scalar fields can be responsible for this stage. In order to know the way we can work with 2 inflaton scalar fields, we will analize the following example.

We consider a chaotic-hybrid potential like

$$V = V_o \left[\left(1 - \frac{\psi}{v^2} \right)^2 + \frac{\phi^2}{\mu^2} + \frac{\phi^2 \psi^2}{\omega^4} \right] \tag{73}$$

In the typical hybrid models, it is spected that the *waterfall* scalar field ψ remain in $\psi = 0$ while the inflaton field ϕ evolve, generating inflation. Then, in a critical value ϕ_c the minimum for $\psi = 0$ become unstable and the waterfall field roll to its true minimum, finishing immediately with the inflationary era. However, there are some works where it is considered that an amount of non-negligible inflation is generated during this transition, that is usually called *waterfall regimen*. If we consider that at the time when $\phi = \phi_c$ the waterfall field is not zero but $\psi = \psi_o$ due to quantum fluctuations, we will have inflation if it is satisfied

$$\epsilon_{\phi_i} = \frac{m_p^2}{16\pi} \left(\frac{V_{,\phi_i}}{V} \right)^2 \ll 1, \quad \eta_{\phi_i \phi_j} = \frac{m_p^2}{8\pi} \frac{V_{,\phi_i \phi_j}}{V} \ll 1, \quad i,j = 1,2 \tag{74a}$$

where $_{,\phi_i} \equiv d/d\phi_i$, and $\phi_1 = \phi$ and $\phi_2 = \psi$. Then, for this two scalar field model, the inflationary parameters are given by

$$n_s - 1 = -6\epsilon_\sigma + 2\eta_{\sigma\sigma} \quad \text{and} \quad r = 16\epsilon_\sigma, \tag{75a}$$

where

$$\epsilon_\sigma = \epsilon_\phi + \epsilon_\psi, \quad \eta_{\sigma\sigma} = \eta_{\phi\phi} \cos^2\theta + 2\eta_{\phi\psi} \sin\theta \cos\theta + \eta_{\psi\psi} \sin 2\theta \tag{75b}$$

and

$$\cos\theta = \frac{\dot\phi}{\sqrt{\dot\phi^2 + \dot\psi^2}}, \quad \sin\theta = \frac{\dot\psi}{\sqrt{\dot\phi^2 + \dot\psi^2}} \tag{75c}$$

Despite this model is similar with the hybrid models, when it is plotted on the $n_s - r$ plane, in the same way that the logaritmic potential, it is located into the small-field region if enough amount of inflation is considering in the waterfall regimen.

6. OBSERVATIONAL REULTS

How can observations constrain n_s and r in inflationary models? During several years many projects at different scales of the Universe, have been carried out in order to look for observational data to constrain cosmological models, that is, different models may imprint different behaviours over the CMB

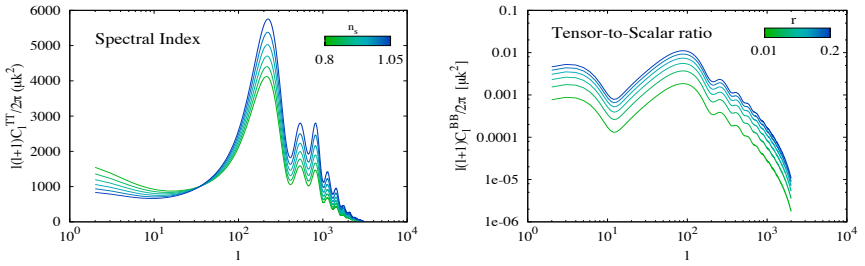

Fig. 9. Variations of the CMB scalar spectrum for different values of the spectral index n_s (left), and variations of the CMB tensor spectrum with respect to the tensor-to-scalar ratio r (right).

spectra, Figure 9. Among many projects, they are: Cosmic Background Explorer (COBE), Wilkinson Microwave Anisotropy Probe (WMAP), Cosmic Background Imager observations (CBI), Ballon Observations of Millimetric Extra-galactic Radiation and Geophysics (BOOMERang), the Luminous Red Galaxy (LRG) subset DR7 of the Sloan Digital Sky Survey (SDSS), Baryon Acoustic Oscillations (BAO), Supernovae (SNe) data, Hubble Space Telescope (HST) and recently the South Pole Telescope (SPT), the Atacama Cosmology Telescope (ACT) and the Planck Satellite. Below, we show some predictions coming from different types of inflationary potentials, comparing them with current observational parameters (Mortonson et al. 2011). We mention some results that have been obtained on the phase space $n_{\rm s} - r$. At this stage, our interest is mainly focussed on the case with no running $dn_{\rm s}/d\ln k = 0$.

Figure 10 displays marginalised posterior distributions for $n_{\rm s}$ and r based on two different types of data sets: WMAP3 by itself, and WMAP3 plus information from the LRG subset from SDSS. Considering WMAP3 observations alone (Kinney et al. 2006), the parameters are constrained such that $0.94 < n_{\rm s} < 1.04$ and $r < 0.60$ (95% CL). Those models which present $n_{\rm s} < 0.9$ are therefore ruled out at high confidence level. The same is applied for models with $n_{\rm s} > 1.05$. WMAP data by itself cannot lead to a strong constraints because the existence of parameter degeneracies, like the well known geometrical degeneracy involving Ω_m, Ω_Λ and Ω_k. However, when it is combined with different types of experiments, together they increase the constraining power and might remove degeneracies. Furthermore, when the SDSS data are included the limit of the gravitational wave amplitude is reduced, whereas the spectral index parameter does not present any relevant change. For WMAP3+SDSS the constraints imposed on $n_{\rm s}$ and r are $0.93 < n_{\rm s} < 1.01$ and $r < 0.31$ (Kinney et al. 2006).

On the other hand, Figure 11 shows that with WMAP5 data alone, $r < 0.43$ (95% CL) while $0.964 < n_{\rm s} < 1.008$. When BAO and SN data are added, the limit improves significantly to $r < 0.22$ (95% CL) and $0.953 < n_{\rm s} < 0.983$.

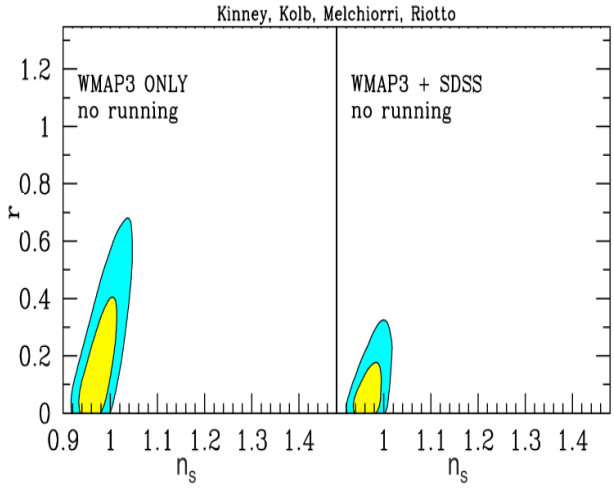

Fig. 10. WMAP3 data sets constraining n_s and r parameters. Coloured regions correspond to 68% and 95% CL (Kinney et al. 2006).

(Komatsu 2009).

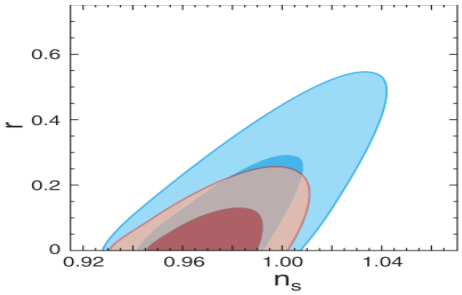

Fig. 11. Constraints on n_s and r. WMAP5 results are coloured blue and WMAP5+BAO+SN red, both on 68% and 95% CL (Komatsu 2009).

Following the same line for inflationary models, we employ the COSMOMC package (Lewis & Bridle 2002) which allows us to produce some predictions for the n_s and r parameters given a dataset. To illustrate our point, we consider WMAP seven year data. We observe from Figure 12, that in order a model to be considered as a favourable candidate it has to predict a small field with spectral index about $n_s = 0.982^{+0.020}_{-0.019}$ and a tensor-to-scalar ratio of $r < 0.37$ (95% CL). When WMAP-7 is combined with different datasets, the constraints are tighten as is shown by (Larson et al. 2011).

Finally in figure 13 the plot for the most resent constrains given by (Planck Colaboration 2015) in the n_s and r plane is shown. In this plot the countour

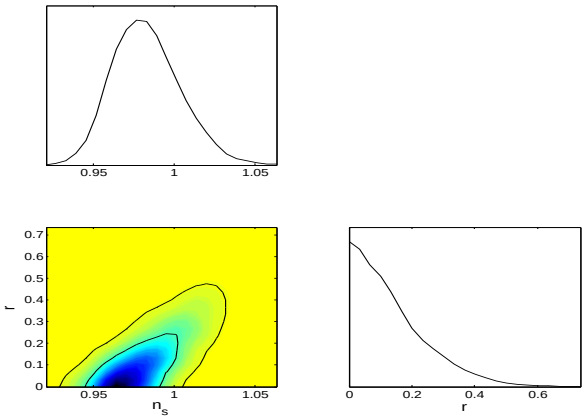

Fig. 12. Marginalised probability constraints on n_s and r using only WMAP7 data. 2D constraints are plotted with 1σ and 2σ confidence contours

regions at the 68% and 95% is presented. Gray regions correspond with the Planck 2013 results, red regions added the contribution of the temperature power spectrum (TT) and the Planck polarization data in the low-l likelihood (lowP) while blue regions added to the red regions the data corresponded to the temperature-polarization cross spectrum (TE) and the polarisation power spectrum (EE).

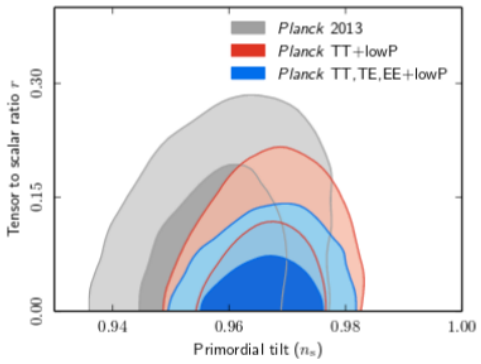

Fig. 13. 2D marginalised probability constraints on n_s and r for the most resent results of (Planck Colaboration 2015). 2D constraints are plotted with 1σ adn 2σ confidence contours. Figure taken from (Planck Colaboration 2015).

7. CONSTRAINTS ON INFLATIONARY MODELS

WMAP3 results are shown in Figure 14. Models with $n_s = 1$ are in a good agreement with CMB data. In particular the Harrison-Zel'dovich model:

$n_s = 1, r = 0, dn_s/d\ln k = 0$, is not ruled out at more than 95% CL from CMB data alone. Similarly, for inflation driven by a massless self-interacting scalar field $V(\phi) = \lambda\phi^4$, the contours indicate that this potential with 60 e-folds is still consistent with the WMAP3 data at 95% CL.

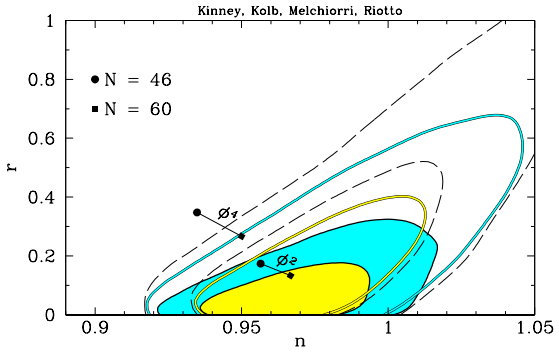

Fig. 14. WMAP3 (open contours) and WMAP3+SDSS (filled contours) constraints on phase space n_s, r. Contours with 68% CL and 95% are shown with dashed lines (Kinney et al. 2006).

On the other hand, WMAP5 results are summarised in Figure 15: The model $V(\phi) = \lambda\phi^4$, unlike WMAP3 constraints, is found to be located far away from the 95% CL, and therefore it is definitely excluded. For inflation produced by a massive scalar field $V(\phi) = (1/2)m^2\phi^2$, the model with $N = 50$ is situated outside the 68% CL, whereas with $N = 60$ is at the boundary of the 68% CL. Therefore, this model for the corresponding number of e-folds is consistent with data within the 95% CL. The points represented by N-flation describe a model with many massive axion fields (Liddle 1998). For an exponential potential, it is observed that models with $p < 60$ are mainly excluded. Models with $60 < p < 70$ are roughly in the boundary of the 95% region, and $p > 70$ are in agreement within the 95% CL. Some models with $p \sim 120$ can be located in or outside the 68% CL, essentially they lay out in the limit.

The hybrid potentials, as was already noted, can have different behaviours depending on the (ϕ/μ) value. The parameter space can be split into three different regions based on (ϕ/μ). For $\phi/\mu \ll 1$ the dynamics is similar to small fields and the dominant term lays in the region called "Flat Potential Regime". For $\phi/\mu \gg 1$ the result is similar to large field models, this region is called "Chaotic Inflation-like Regime". The boundary, $\phi/\mu \sim 1$ is named "Transition regime". The different (ϕ/μ) values corresponding to their regions are shown in Figure 15.

Two recent experiments have placed new constraints on the cosmological parameters: the Atacama Cosmology Telescope (ACT; Dunkley et al. (2010)) and the South Pole Telescope (SPT; Keisler et al. (2011)). Figure 16 shows

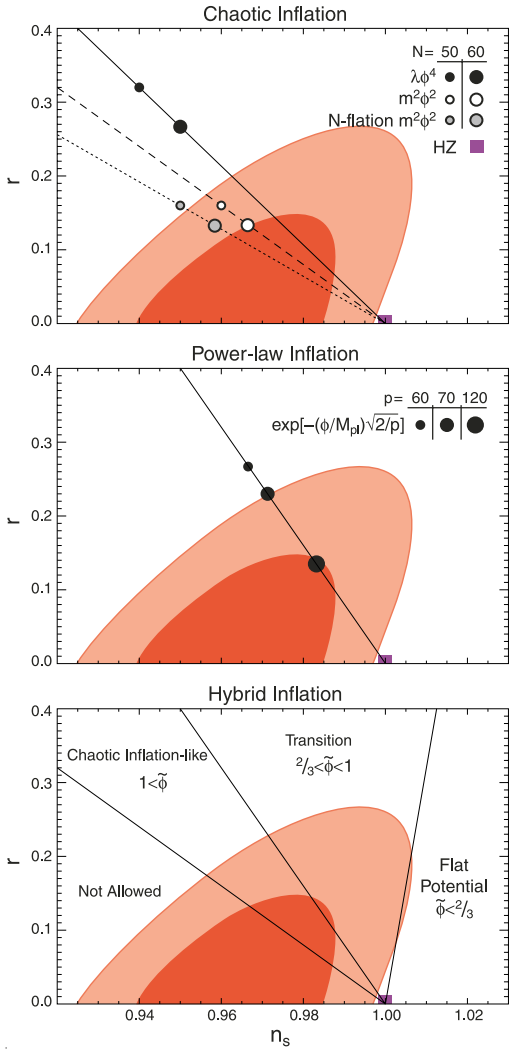

Fig. 15. Constraints on large and hybrid models obtained from WMAP5+BAO+SN. They are shown in contours with 68% and 95% CL (Komatsu 2009).

the predicted values for a chaotic inflationary model with inflaton potential $V(\phi) \propto \phi^p$ with 60 e-folds. We observe that models with $p \geq 3$ are disfavored at more than 95% CL.

8. CONCLUSIONS

Considering the analysis presented here is complicated to prove that a given model is correct, since these could be just particular cases of more general models with several parameters involved. However, it is possible to eliminate models or at least give some constraints on their behaviour leading to a narrower range of study.

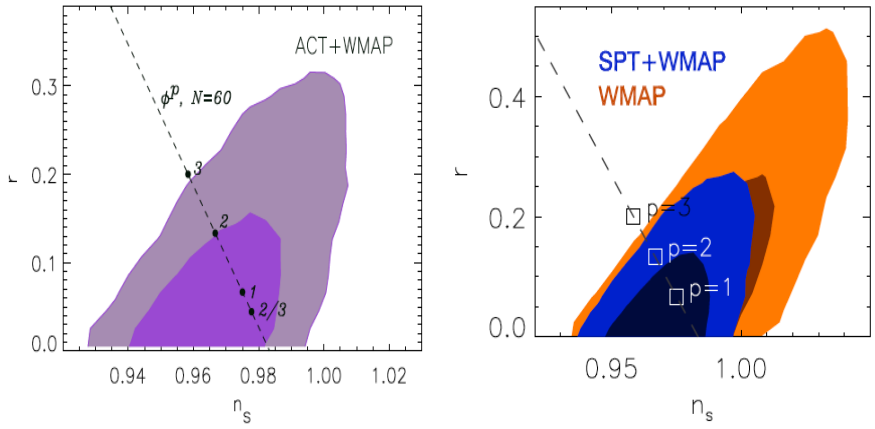

Fig. 16. Marginalized 2D probability distribution (68% and 95% CL) for the tensor-to-scalar ratio r, and the scalar spectral index n_s for ACT+WMAP (left panel) and SPT+WMAP (right panel) (Dunkley et al. 2010; Keisler et al. 2011).

Although we have presented some simple examples of potentials, the classification in small-field, large-field, and hybrid models is enough to cover the entire region of the n_s–r plane as illustrated in Figure 8. Different versions of the three types of models predict qualitatively different scalar and tensor spectra, so it should be particularly easy to work on them apart.

We have seen that, the favoured models are those with small r (for $dn_s/d\ln k \sim 0$) and slightly *red* spectrum, hence models with *blue* power spectrum $n_s > 1.001$ are inconsistent with the recently data. This simple but important constraint allows us to rule out the simplest models corresponding to hybrid inflation of the form $V(\phi) = \Lambda^4(1 + (\mu/\phi)^p)$. There still remain models with red spectra in the hybrid classification: inverted models and models with logarithmic potentials.

Scale-invariant power spectrum $n_s = 1$ is consistent within 95% CL with WMAP3 data alone, considering no running of the spectral index. The HZ spectrum is therefore not ruled out by WMAP3. However, considering WMAP5 data, Figure 15 shows that HZ spectrum lays outside the 95% CL region, which indicates it is excluded considering the lowest order on the n_s, r parameters. When WMAP7 data without tensors is considered, scale-invariant spectrum is totally excluded by more than 3σ, however the inclusion of extra parameters weaken the constraint on the spectral index, in which case certain models are still consistent with HZ even for current observations. When chaotic models $V(\phi) \propto \phi^p$ are analysed with current data, it is found that quartic models ($p = 4$) are ruled out, whilst models with $p \geq 3$ are disfavoured at $> 95\%$ CL. Moreover, the quadratic potential $V(\phi) = 1/2m^2\phi^2$ is in agreement with all data sets presented here and therefore remains as a

TABLE 1

SUMMARISE OF THE $n_{\rm s}$, r CONSTRAINTS FROM DIFFERENT MEASUREMENTS [a].

Parameter	Limits	Data set
$n_{\rm s}$	0.968 ± 0.006	PLANCK (idealised)
r	< 0.15	
$n_{\rm s}$	0.9711 ± 0.0099	SPT+WMAP7+BAO+H_0
r	< 0.17	
$n_{\rm s}$	0.970 ± 0.012	ACT+WMAP7+BAO+H_0
r	< 0.19	
$n_{\rm s}$	0.973 ± 0.014	WMAP7 + BAO +H_0
r	< 0.24	
$n_{\rm s}$	$0.982\pm^{+0.020}_{-0.019}$	WMAP7 ONLY
r	< 0.36	
$n_{\rm s}$	0.968 ± 0.015	WMAP5+BAO+SN
r	< 0.22	
$n_{\rm s}$	0.986 ± 0.022	WMAP5 ONLY
r	< 0.43	
$n_{\rm s}$	0.97 ± 0.04	WMAP3 + SDSS
r	< 0.31	
$n_{\rm s}$	0.99 ± 0.05	WMAP3 ONLY
r	< 0.60	

[a]Peiris et al.2003; Kinney et al.2006; Komatsu et al.2009; Komatsu et al.2011; Dunkley et al. 2010; Keisler et al. 2011

good candidate. Table 1 summarises the constraints on the $n_{\rm s}$ and r parameters and its improvements through the years. Future surveys will provide a more accurate description of the universe and therefore narrow the number of candidates which might better explain the inflationary period.

9. ACKNOWLEDGMENTS

JAV was supported by CONACyT México.

REFERENCES

Albrecht, A., and Steinhardt, P. J. 1982, Phys. Rev. Lett., 48, 1220
Ambrosio, M., et al. 2002, Eur. Phyis. J. C., 25, 511
ASTROPHYSICAL CONSTANTS AND PARAMETERS, *http* : *//pdg.lbl.gov/*2016/*reviews/rpp*2016 − *rev* − *astrophysical* − *constants.pdf*, revised December 2017
Barrow, J. D., and Parsons, P. 1995, Phys. Rev. D, 52, 10

Barrow, J. D., Tipler, F. J., 1986, The Anthropic Cosmological Principle, Clarendon Press, Oxford, UK
Baumann, D., and Peiris, H. V. 2009, Adv. Sci. Lett., 2, 105
C. D. McCoy, What Is the Horizon Problem?, november 2014
Carroll, S. 2001, Living Rev. Relativity, 3
Coles, P., and Lucchin, F. 1995, Cosmology, WILEY, England, UK
Copeland, E. J., et al. 1994, Phys. Rev. D, 49, 6410
Dodelson, S. 2003, Modern Cosmology, Academic Press, Amsterdam, Netherlands
Dunkley, J., et al. 2010, astro-ph/1009.0866.
Georgi, H., Glashow, S. L. 1974, Phys. Rev. Lett., 32, 438
Gold, B., et al. 2011, ApJS, 192, 15
Guth, A. H. 1997, The Inflationary Universe, Ed. Vintage
Guth, A. H. 1981, Phys. Rev. D, 23, 347
Hu, W., and Dodelson, S. 2002, Annu. Rev. Astron. and Astrophys., 40, 171
Hinshaw, G., et al. 2009, ApJS, 180, 225
Keisler, R., et al. 2011, astro-ph/1105.3182
Kinney, W . H. 2004, CU-TP-1083, astro-ph/0301448
Kinney, W. H., et al. 2006, Phys. Rev. D, 74, 023502
Kinney, W. H., and Riotto, A., 1998, Phys. Lett., 435B, 272
Kolb, E. W., Turner, M. S. 1983, Ann Rev Nucl Part Sci. 33, 645
Kolb, E. W., Turner, M.S. 1994, The Early Universe, Westview Press
Komatsu, E., et al. 2009, ApJS., 180, 330
Komatsu, E., et al. 2011, Astrophys. J. Suppl., 192, 18
La, D., and Steinhardt, P.J. 1999, Phys. Rev. D, 59, 064029
Larson, D., et al. 2011, ApJS., 192, 16
Lewis A., and Bridle, S., 2002, Phys. Rev D, 66, 103511
Liddle, A. 1999, AIP Conf. Proc., 476, 11
Liddle, A., Mazundar, A., and Schunck, F. E. 1998, Phys. Rev. D, 58, 061301
Liddle, A. 1999, An introduction to Modern Cosmology, WILEY, England, UK
Liddle, A. R., and Lyth, D. H. 2000, Cosmological inflation and large-scale structure, Cambridge University Press, Cambridge, UK
Liddle, A. R., and Lyth, D. H. 2009, The primordial density perturbation, Cambridge University Press, Cambridge, UK
Liddle, A.R. and Lyth, D.H 1992, Phys. Lett. B, 291, 39
Liddle, A. R., et al. 1994, Phys. Rev. D, 50, 12
Linde, A. D. 1982, Phys. Lett. B, 108, 389
Linde, A. D. 1983, Phys. Lett. B, 129, 177
Linde, A. D. 1990, Particle Physics and Inflationary Cosmology, Harwood Academic, Switzerland
Linde, A. D. 1991, Phys. Lett. B, 259, 38
Linde, A. 2005, J.Phys.Conf.Ser., 24
Lidsey, J. E., et al. 1997, Annu. Rev.Mod.Phys., 69, 373
Lyth, D. H., and Riotto, A. 1999, Physics Reports, 314, 1
Lyth, D. H., and Stewat, E. D., 1995, Physics Rev. Lett. 75, 201, hep-ph/9502417
Lyth, D. H., and Stewat, E. D., 1996a, Physics Rev. D 53, 1784, hep-ph/9510204
Mortonson, M. J., Peiris, H.V., and Easther, R. 2011, Phys.Rev. D, 83, 043505
Mukhanov, V. F., and Chibisov, G. V. 1997, JETP Letters, 33, 532
Olive, K. A. 1990, Physics Reports, 190, 307
P. A. R. Ade et al. Planck collaboration. Astron. Astrophys. 594, A20 (2016). arXiv:1502.02114 [astro-ph.CO]. doi: 10.1051/0004-6361/201525898
P. Mermod, *Magnetic monopoles at the LHC in the Cosmos*, arXiv:1305.3718 [hep-ex]
Peiris, H. V., et al. 2003, ApJS., 148, 213
Planck 2015 results. XI. CMB power spectra, likelihoods, and robustness of parameters, DOI: 10.1051/0004-6361/201526926, arXiv:1507.02704 [astro-ph.CO]
Planck 2015 results. XIII. Cosmological parameters, arXiv:1502.01589 [astro-ph.CO]
Planck 2015 results. XVI. Isotropy and statistics of the CMB, DOI: 10.1051/0004-6361/201526681, arXiv:1506.07135v2 [astro-ph.CO]

The Planck Collaboration, 2016, astro-ph/0604069.
Riess, A. G., et al. 2009, ApJ., 699, 539
Smooth, G. F., et al. 1992, ApJ Letters, 396, L1
Springel, V., et al. 2005, Nature, 435, 629
Tegmark, M., et al. 2001, Phys. Rev. D, 63, 043007
The LIGO Scientific Collaboration and The Virgo Collaboration, *A gravitational-wave standard siren measurement of the Hubble constant*
Vilenkin, A., Shellard, E. P. S. 2000, Cosmic Strings and Other Topological Defects, Cambridge University Press, Cambridge, UK

J. Alberto Vázquez: Kavli Institute for Cosmology, Madingley Road, Cambridge CB3 0HA, UK.
Astrophysics Group, Cavendish Laboratory, JJ Thomson Avenue, Cambridge CB3 0HE, UK. (jv292@cam.ac.uk)

Luis E. Padilla: Departamento de Física, Centro de Investigación y de Estudios Avanzados del IPN, AP 14-740,07000 México D.F., México. (epadilla@fis.cinvestav.mx)

Tonatiuh Matos: Departamento de Física, Centro de Investigación y de Estudios Avanzados del IPN, AP 14-740,07000 México D.F., México. (tmatos@fis.cinvestav.mx)